
This is an electronic reprint of the original article.
This reprint may differ from the original in pagination and typographic detail.

Kiil, Martin; Valgma, Indrek; Võsa, Karl Villem; Simson, Raimo; Mikola, Alo; Tark, Teet; Kurnitski, Jarek

Ventilation effectiveness in classroom infection risk control

Published in:
E3S Web of Conferences

DOI:
[10.1051/e3sconf/202339601043](https://doi.org/10.1051/e3sconf/202339601043)

Published: 16/06/2023

Document Version
Publisher's PDF, also known as Version of record

Published under the following license:
CC BY

Please cite the original version:
Kiil, M., Valgma, I., Võsa, K. V., Simson, R., Mikola, A., Tark, T., & Kurnitski, J. (2023). Ventilation effectiveness in classroom infection risk control. *E3S Web of Conferences*, 396, Article 01043.
<https://doi.org/10.1051/e3sconf/202339601043>

Ventilation effectiveness in classroom infection risk control

Martin Kiil^{1*}, Indrek Valgma¹, Karl-Villem Võsa¹, Raimo Simson^{1,2}, Alo Mikola¹, Teet Tark¹, Jarek Kurnitski^{1,2}

¹ Department of Civil Engineering and Architecture, Tallinn University of Technology, Tallinn, Estonia

² Department of Civil Engineering, Aalto University, Espoo, Finland

Abstract. The benefits of a good ventilation in classrooms are a well-studied topic regarding health and learning outcomes. However, many studies still show poor results regarding air quality, air change rate and air velocities. In this paper, typical Estonian classroom air distribution solutions were studied in an air distribution laboratory at Tallinn University of Technology. The air change efficiency was measured with CO₂ tracer gas concentration decay method. For determining the contaminant removal effectiveness, continuous dose method was used to create a constant contaminant source. In addition, by using air velocity probes, we conducted draught measurements in the mock-up classroom. Tests were conducted using dedicated room-based air handling unit and thermal mannequins for imitating heat sources from students. We found that all solutions studied ensured the air change efficiency roughly corresponding to fully mixing air distribution, but local ventilation effectiveness values of contaminant removal showed large variation from 0.6 to 1.7 stressing the impact of source location. Grouped ceiling supply circular diffusers and single vertical supply grille air distribution commonly used in renovated educational buildings resulted in higher draught risk on the border of the occupied zone. High air velocities recorded in some areas of the classroom perimeter, well explain why draught is considered as one of the main reasons why the airflow rates are reduced, or supply air temperatures are lifted compared to designed values. Perforated duct diffusers resulted in acceptable air velocities. In conclusion, local ventilation effectiveness of contaminant removal showed that fully mixing is not a case with a point source, although air change efficiency determined with equally distributed source showed fully mixing conditions. Therefore, in those cases, the air change rate should be increased to achieve the same ventilation effectiveness. Based on the experiments conducted, a point source ventilation effectiveness measurement method for the breathing zone is proposed. This value determined at least with two source locations can be used in infection risk-based ventilation design.

Keywords. Classroom, ventilation effectiveness, air velocity

1 Introduction

Studies have shown that poor indoor air quality in classrooms reduces students' performance and has a negative impact on the health. Inadequate ventilation increases the risk of asthma symptoms, absenteeism and respiratory disease among students [1–6]. Proper air change rates are found to ensure better results [7–10]. Air distribution plays a significant role in ensuring air quality, which determines how efficiently the contaminated air in the room is replaced with fresh, clean air.

Using carbon dioxide (CO₂) as a tracer gas for evaluating ventilation effectiveness is well validated [11–15]. The main alternative to the measuring techniques is to CFD simulate air distribution and quality. Ventilation strategies were studied by Novoselac and Srebic [16], indicating that overlapping results in the occupied zone and breathing plane lower the total number of necessary measurement points. Kosonen and Mustakallio [17,18] analysed mixing and displacement ventilation concepts in a mock-up classroom with follow-up CFD-simulations concluding

that heat gains in rooms with mixed air exchange may have a significant effect on the air distribution and draught. Lichtner and Kriegel [19] studied classroom ventilation in the view of the Covid-19 pandemics. The CFD-simulations indicated air quality in the breathing plane up to five times worse than expected. Strong correlation between ventilation strategy and airborne transmittable diseases is emphasised also by other studies [20,21]. However, mixing air distribution is the oldest and most common solution, the purpose of which is to ensure the most uniform removal of pollutants and temperature distribution in the occupied zone [22,23]. Furthermore, a new infection risk-based ventilation design method [24] was recently introduced. Infection-risk based ventilation equations apply for fully mixing and need to be divided by point source ventilation effectiveness for actual air distribution solutions [25].

The focus of this paper is to evaluate ventilation effectiveness simultaneously with draught risk in a mock-up classroom. Ventilation effectiveness indices and air velocities are presented. Main findings of the experiments indicate that the ventilation solutions do not always guarantee the expected efficiency, or the air velocities do not maintain the required limits in the occupied zone.

* Corresponding author: martin.kiil@taltech.ee

Nomenclature

ε^a	air change efficiency, %	ε_b	point source ventilation effectiveness for the breathing zone, -
ε_p^a	local air change index, %	t_i	indoor air temperature, °C
$\varepsilon^c = CRE$	contaminant removal effectiveness, -	t_{sup}	supply air temperature, °C
ε_p^c	local air quality index, -	v_a	air velocity, m/s
ε_b^j	point source ventilation effectiveness of measurement j , -		

2 Methods

This chapter provides information regarding ε^a , CRE and v_a measurements with the description of the ventilation laboratory used in the experiments. The research methodology flow chart is seen on Figure 1. Using air distribution laboratory at the campus of

Tallinn University of Technology, a mock-up classroom was set up for the experiments. Measuring equipment data is provided below in the second subsection of this chapter. The principles of the analysis based on the results of the carried-out experiments are described at the end of this chapter. SciPy and matplotlib software libraries in the Python programming language were used for visualisation of the results.

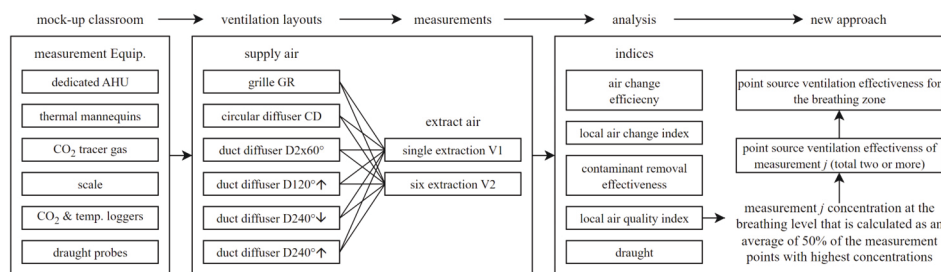


Figure 1. Flow chart of research methodology.

2.1 Mock-up classroom

The tests were conducted in an open ceiling mock-up classroom with a room height of 3.8 m and floor area of 5.2×8.7 m (45 m²). For 29 students and one teacher the required air change 240 l/s (5.3 l/s×m², 5 l/h) was used [26]. The ventilation layouts used in the experiments are

shown in Figure 2. The tests included ceiling diffusers, grille, and duct diffusers. The experiments included extract with individual location and with 6 points distributed evenly over the room. The indoor air and supply air temperatures during measurements were respectively $t_i = +22$ °C and $t_{sup} = +18$ °C using a dedicated air handling unit.

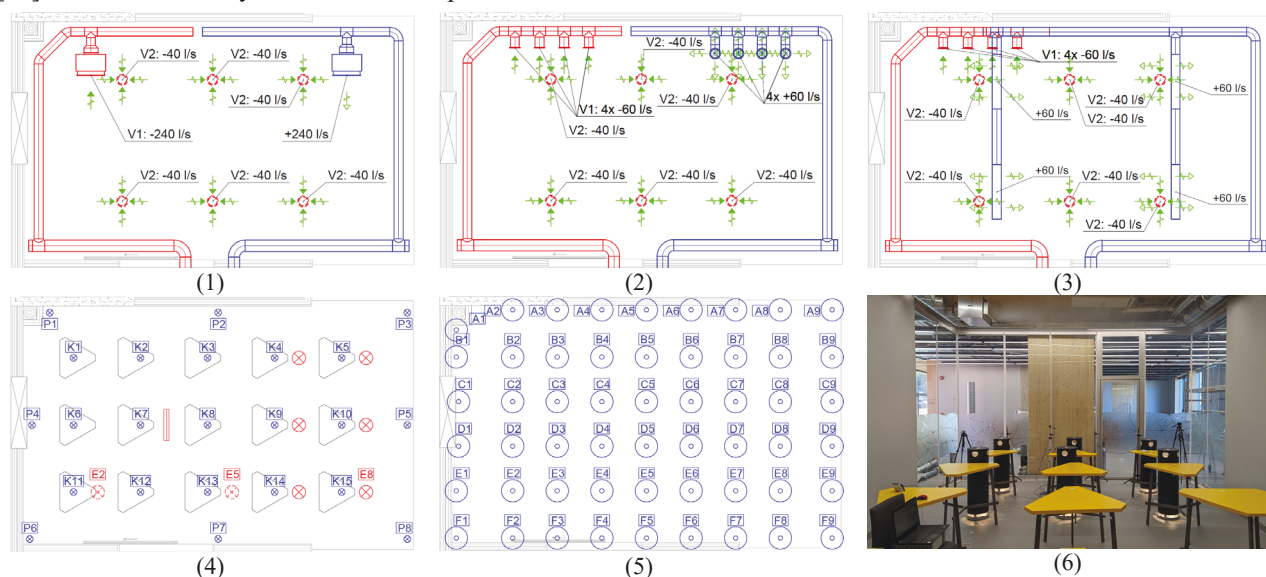





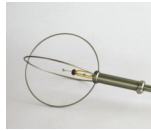
Figure 2. Ventilation layouts and measurement equipment used in the experiments: (1) grille, (2) circular diffuser, (3) duct diffuser, (4) “K” and “P”-labelled data loggers for occupied zone and room perimeter with the location of thermal mannequins (E2, E5 and E8 as contaminant source), (5) draught probes’ measurement points (A1 to F9) and (6) photo of the mock-up classroom. V1 and V2 in the (1) to (3) layouts represent single and six extraction options.

2.2 Measurement equipment

To assess ε^a and CRE , we used CO_2 as a tracer gas respectively for concentration decay method and continuous dose method. To measure CO_2 concentrations, calibrated dataloggers were used: 15 on the tables (breathing plane, $h=1.1$ m), 8 in the perimeter ($h=1.1$ m), 1 in supply air duct for fresh air reference concentration and 1 in extraction duct for single location extract and 6 for multiple extract point layout (see

Figure 2). For measuring gas dosage, scale was used. Air diffusers were balanced and measured for each layout using differential pressure manometer. In addition, to assess draught risk, each ventilation layout was measured as a level ($h=1.1$ m) by a set of 6 air velocity (v_a) probes with 1 m step. The experiments were conducted with t_i of $+22.7 \pm 0.8$ °C and t_{sup} of $+19.9 \pm 0.7$ °C, maintaining an Δt of t_i and t_{sup} with ~ 4 K. The specifications of measuring equipment are provided in Table 1.

Table 1. Specifications of measuring equipment : CO_2 concentration and temperature logger [27], differential pressure sensor [28], gas mass weighing scale [29], draught probe [30].

	Onset HOBO MX1102A Data Logger	Testo 440 dP	Kern FKB	Draught probe ComfortSense 54T35
Parameters	CO_2 concentration air temperature	differential pressure	weight	air velocity air temperature
Range	0...5000 ppm 0...50 °C	-150 to +150 hPa	0.002...65 kg	0.05-5 m/s -20 °C to +80 °C
Accuracy	± 50 ppm + ± 5 % ± 0.21 °C	<100 Pa ± 0.05 Pa	± 0.001 kg	± 0.02 m/s ± 0.2 K
Image				

The placement of thermal mannequins and one extra 1 kW electrical convector are seen in Figure 2. Before the ε^a assessment experiments, the room was filled with gas to fully mixed state. However, during CRE experiments, gas was injected as a contaminant continuously during the test. We used CO_2 tank connected to a dummy as a contaminant source (Figure 3) in three different positions.

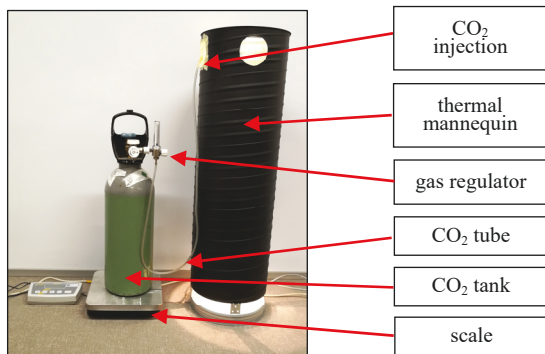


Figure 3. CO_2 tank connected with a thermal mannequin used as a contaminant source.

2.3 Data analysis of ventilation effectiveness

The ventilation effectiveness indicates the potential of a system to exchange the air in the room or to remove airborne contaminants. Therefore, the first is subdivided to air change efficiency (ε^a) and local air change index (ε_p^a). Thus, the second is subdivided to contaminant removal effectiveness (ε^c) and local air quality index (ε_p^c). Another useful tool for evaluating ventilation effectiveness in the age of air. The local mean age of air ($\bar{\tau}_p$) is always equal to the nominal time constant (τ_n) in the exhaust, which can be found using Equation 1. [11]

$$\tau_n = V / q_v, (\text{h}) \quad (1)$$

where V stands for room volume and q_v as the air change rate. Using the ratio (Equation 2) between the lowest possible mean age of air and the actual room mean age of air, ε can be calculated. [11]

2.3.1 Calculating air change efficiency

The Equation 2' upper limit is 100 % in a piston flow situation. Between 50 % and 100 %, displacement flow is considered, while 50 % equals fully mixed flow and under 50 % efficiency indicates a short-circuit flow. [11]

$$\varepsilon^a = \frac{\tau_n}{2(\bar{\tau})} \times 100, (\%) \quad (2)$$

Calculating conditions in a particular point, Equation 3 must be used, where $\bar{\tau}_p$ represent the local mean age of air: [11]

$$\varepsilon_p^a = \frac{\tau_n}{\bar{\tau}_p} \times 100, (\%) \quad (3)$$

Determining airflow rates with traces gas dilution method is described in EN ISO 12569:2017 [14]. Methods for characterization of ventilation conditions with local mean ages of air is provided in ISO 16000-8:2007 [15]. Following procedure of multi-point concentration decay method, Equation 4 was used:

$$N = \frac{(\sum_{j=1}^{np} t_j) \times \sum_{j=1}^{np} \ln C(t_j) - n_p \times \sum_{j=1}^{np} t_j \times \ln C(t_j)}{n_p \times \sum_{j=1}^{np} t_j^2 - (\sum_{j=1}^{np} t_j)^2}, \quad (4)$$

where N stands for air change rate (1/h), t_j is a cumulative time step from the start of the experiment ($t_i = 0$, h), $C(t_j)$ represents the traces gas concentration at a time step j (ppm) and np shows the sum of measuring points. Finally, using Equation 5, local mean age of air is calculated as an inverse value of local air change rate (λ , 1/h) [15].

$$\bar{\tau}_p = \frac{1}{\lambda}, (\text{h}) \quad (5)$$

2.3.2 Calculating contaminant removal effectiveness

Using ratio (Equation 6) between the steady state concentration (c_e) and the steady state mean concentration of the room ($\langle c \rangle$), ventilation effectiveness of contaminant removal (ε^c) can be calculated. While as Equation 7 was used to calculate ε_p^c , where represents the concentration of contaminant at the point P. On both cases, supply air concentration c_{sup} is subtracted from extract air concentration c_{ext} and from mean concentration $\langle \bar{c} \rangle$ (Equation 6) or local concentration c_p (Equation 7) [11]. According to EN 16798-3:2017 [31], Equation 6 is called ventilation effectiveness.

$$\varepsilon^c = \frac{c_e}{\langle c \rangle} = \frac{(c_{ext} - c_{sup})}{(\langle \bar{c} \rangle - c_{sup})}, (-) \quad (6)$$

$$\varepsilon_p^c = \frac{c_e}{c_p} = \frac{(c_{ext} - c_{sup})}{(c_p - c_{sup})}, (-) \quad (7)$$

2.3.3 Calculating ventilation for infection risk

Breathing zone ventilation rate ($q_{V,bz}$) divided with ventilation effectiveness (ε^c) from Equation 6 represents the ventilation outdoor air volume flow needed at the room supply diffusers, Equation 8:

$$q_{V,ODA} = \frac{q_{V,bz}}{\varepsilon^c}, (\text{m}^3/\text{s}) \quad (8)$$

Breathing zone ventilation rate ($q_{V,bz}$) can be calculated as the infection risk-based ventilation rate as shown in [24]. The main aim of this paper is to provide information about ε^c values in classrooms. Instead of the breathing zone mean concentration (Equation 6) we use local breathing zone values (Equation 7). In the case of the point source (an infectious person) the latter should be used as the denominator in the Equation 8, to apply the formula in the new infection risk-based design method [24] recently proposed. The latter in turn has been supplemented with quanta emission input data to simplify the ventilation rate (Q) calculation directly for common room types as design ventilation airflow rate at actual air distribution solution (Q_s)[25] as in Equations 9 to 11:

$$Q_s = \frac{Q}{\varepsilon_b}, (\text{l/s}) \quad (9)$$

Table 2. Results of calculated air change efficiency (ε^a) and local air change index (ε_p^a), calculated ventilation effectiveness of contaminant removal (ε^c) and point source ventilation effectiveness of measurements with positions of 1-3 (ε_b^j) with point source ventilation effectiveness (ε_b), and measured air velocity (v_a) for grille (GR), circular diffuser (CD), and downward 240° duct diffuser (D240°↓) supply comparing single (V1) and six (V2) extraction layouts in the occupied zone on the breathing plane.

Experiment	Air change efficiency, local air change index			Contaminant removal effectiveness, point source ventilation effectiveness for the breathing zone						Average point source ventilation effectiveness	Air velocity	
				Position 1 (E2)		Position 2 (E5)		Position 3 (E8)				
	ε^a %	$\varepsilon_{P,min}^a$ %	$\varepsilon_{P,max}^a$ %	ε^c -	ε_b^1 -	ε^c -	ε_b^2 -	ε^c -	ε_b^3 -	ε_b -	v_a m/s	$v_{a,max}$ m/s
GRV1	51	92	107	1.06	0.88	1.07	0.85	1.06	0.98	0.90	0.09	0.40
GRV2	50	94	106	0.90	0.65	0.98	0.82	1.09	1.03	0.83		
CDV1	50	97	106	1.73	1.51	1.62	1.39	1.20	1.12	1.34	0.10	0.31
CDV2	51	94	107	1.34	1.17	1.23	1.01	1.05	0.97	1.05		
D240°↓V1	56	107	124	1.09	1.02	0.97	0.87	0.87	0.82	0.91	0.11	0.21
D240°↓V2	50	94	106	1.09	1.03	1.00	1.00	0.99	0.98	1.00		

where ε_b stands for point source ventilation effectiveness for the breathing zone:

$$\varepsilon_b = \frac{\sum_j \varepsilon_b^j}{m}, (-) \quad (10)$$

where ε_b^j represents point source ventilation effectiveness of measurement j . Henceforth, the ε_b^j differs from ε_p^c (Equation 7) in that:

$$\varepsilon_b^j = \frac{c_{je} - c_{jo}}{c_{jb} - c_{jo}}, (\text{l/s}) \quad (11)$$

where c_{je} represents measurement j concentration in the extract air duct (c_{ext}), c_{jb} represents measurement j concentration at the breathing level that is calculated as an average concentration of 50% of the measurement points having the highest concentrations, c_{jo} represents concentration in the supply air (c_{sup}) and m means the total number of measurements (two or more) with different point source locations.

Results and discussion

In this section, the main results of the experiments conducted are provided and discussed. Not all the ventilation layout options provided in Figure 1 are reported in the results. Duct diffusers with horizontal 2x60°, upward (↑) 120°, and 240°↑ settings did not perform as well as downward (↓) 240° version regarding ε_b values. The duct diffuser setting with 120°↓ showed air velocities up to 0.45 m/s in the occupied zone. We noticed that increasing the supply air temperature to the room air temperature level did not reduce the performance of these ventilation solutions significantly. The results of calculated ε^a with minimum and maximum ε_p^a , calculated ε^c with ε_b (calculated from ε_p^c values), and measured v_a values, all without perimeter, are provided in Table 2. The results of calculated ε_p^a as colour-maps are provided in Figure 4 and the results of ε_p are reported in Figure 5. Measured values of v_a are seen below on Figure 6.

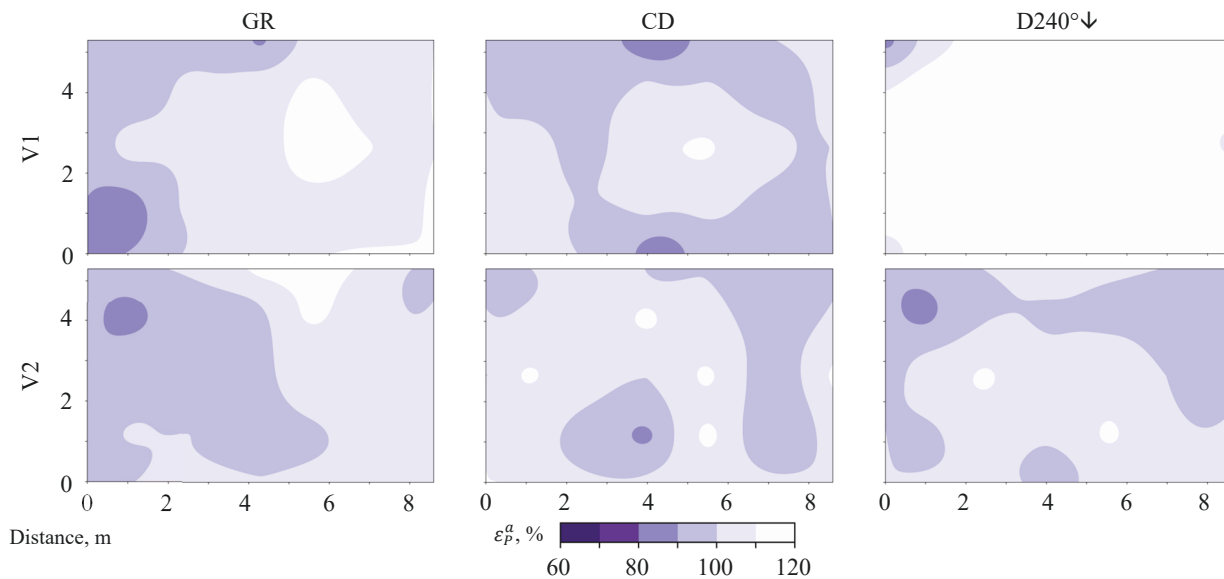


Figure 4. Results of calculated local air change index (ε_p^a) representing mock-up classroom breathing plane colour-maps from CO₂ concentration decay method measurements. Grille (GR), circular diffuser (CD), and duct diffuser (D240°↓) compared with single (V1) and six (V2) extraction (for measurement grid and equipment, see Figure 2).

In all cases, the ε^a results show equivalent values to the theoretical mixing ventilation value of 50%. The lowest values for $\varepsilon_{p,min}^a$ were calculated 92% according to the measurements. Duct diffuser option with single extraction can be highlighted with both better air change efficiency and local air change index. In general, except for the last-mentioned case, as seen on Figure 4, ε_p^a is comparably uniform with other layout settings. Thus, according to the Equation 8 and the average ε^a results indicating mixing ventilation situation ($\varepsilon^a = 50\%$), increasing of the air change rate would not be needed.

Comparing ε^c results, better contaminant removal effectiveness is achieved on all cases, when contaminant source is positioned in the middle P2 (E5) of the classroom. The results presented in the middle column in the Figure 5 show slight symmetry, if at all. In general, grille with six extraction layout in P3 (E8), all the circular diffuser and both P1 (E2) duct diffuser settings stand out with less spreading of the “contaminant”. In the middle position P2 (E5), CO₂ concentration was measured slightly more distributed around the source in case of duct diffuser layouts. The outspread becomes more diffusing for grille option, except for P3 (E8) with six extraction option, as mentioned earlier. The most critical areas are measured for duct diffuser settings with contaminant source positioned in P3 (E8). Left P1 (E2) position shows 0.90 and right P3 (E8) position shows 0.87 for ε^c with grille (GR) with six extraction (V2) and duct diffuser (D240°↓) with single extraction (V1) respectively.

However, ε_b results for positions 1 to 3 are more varying together with middle P2 (E5) position not having an advantage. The lowest point source ventilation effectiveness for position P1 (E2) is 0.65 with grille and six extraction, for position P2 (E5) 0.82 with grille and six extraction (0.85 with one extraction)

and for position 3 (E8) the least value dropped to 0.82 with duct diffuser and single extraction layout. In terms of better performance, for position P1 (E2), circular diffuser with single extract achieved ε_b 1.51. Position 2 (E5) follows with 1.39 and position 3 (E8) with 1.12.

Similarly, to the comparison of the general ventilation efficiency according to the Equation 8 in the mock-up classroom with ε^a , mixing ventilation occurs with $\varepsilon^c = 1$. Therefore, in position 1 (E2), the ventilation rate should be increased by 11% for the grille and six extract layout ($\varepsilon^c = 0.90$). For position 2 (E5), lower ε^c values can be rounded up to 1. If duct diffuser single extract solution $\varepsilon^c = 0.87$ could be rounded to 0.9, again ventilation rate should be increased by 11%. In the case of duct diffuser, the ventilation rate can be reduced.

Hence, according to ε_b , the ventilation rates should be adjusted up to 14% ($\varepsilon_b = 0.88$ in P1) in case of grille with single extract and up by 54% ($\varepsilon_b = 0.65$ in P1) in case of six extraction. Less conservative would be to use average value of three contaminant source positions, 0.90 and 0.83 respectively, with the need of higher ventilation rate by 11% and 20%. In case of duct diffusers, the same approach would indicate 22% ($\varepsilon_b = 0.82$ in P3) demand for ventilation increase with single extract and 2% ($\varepsilon_b = 0.98$ in P3) for six extract. The less conservative average values based on three contaminant source positions would be 0.91 and 1.00 with the need for ventilation rate increase of 10% and no need respectively. Therefore, using ε_b values instead of ε^c as a correction factor for dimensioning ventilation rate, presuming mixing ventilation, would be preferred. It is likely enough conservative to use an average of the two or more measurement positions ε_b values and not the random single nor the lowest measurement ε_b value available which may result in excessive over dimensioning of the ventilation rate.

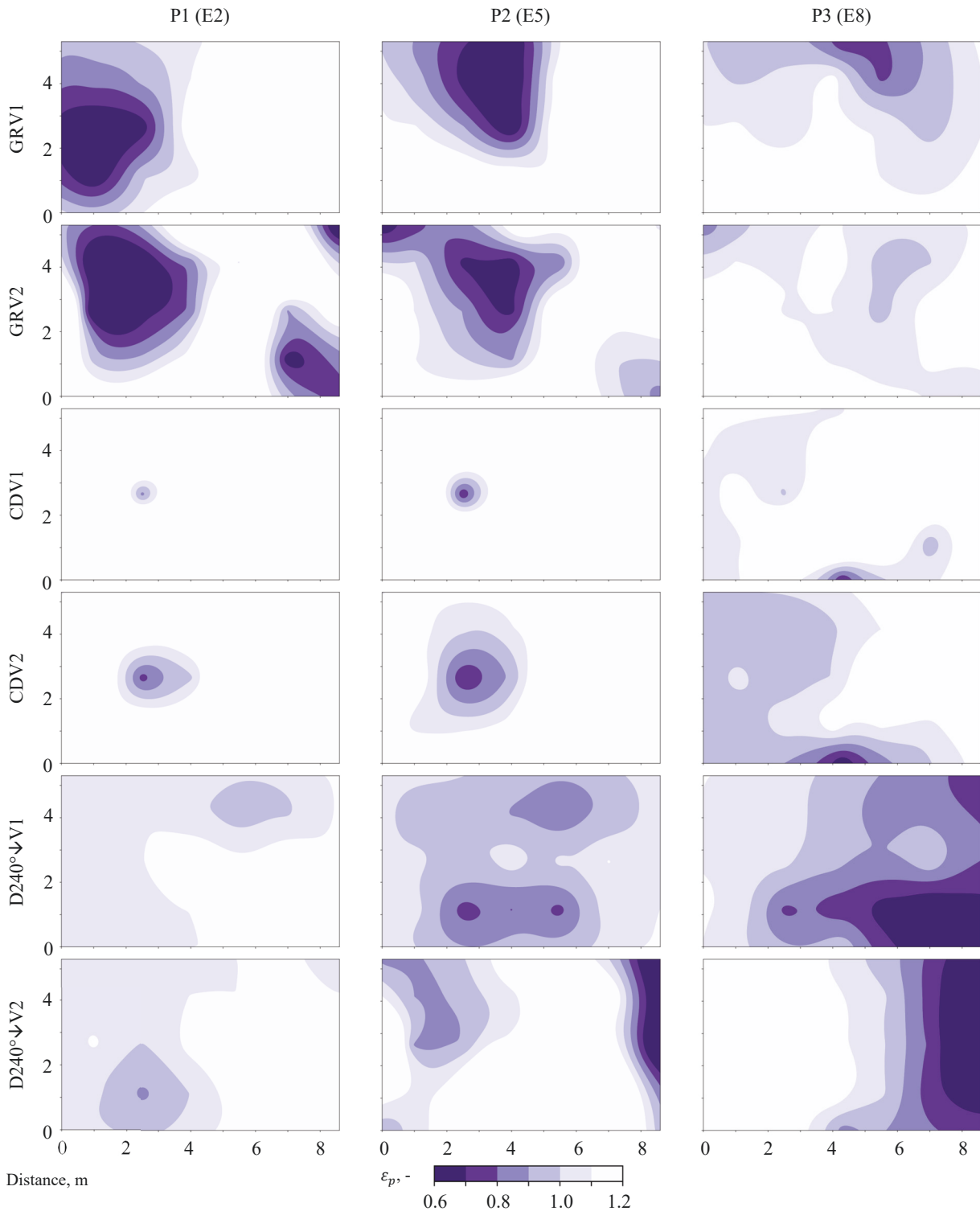


Figure 5. Measured local air quality index (ϵ_p) from which point source ventilation effectiveness can be calculated, representing mock-up classroom breathing plane colour-maps from continuous injection method. Grille (GR), circular diffuser (CD), and duct diffuser (D240°V) compared with single (V1) and six (V2) extraction for each contaminant source position P1-P3 (for measurement grid and equipment, see Figure 2).

The Category I, II, and III air velocities are 0.10, 0.16, and 0.21 m/s during winter and 0.12, 0.19, and 0.24 m/s during summer respectively [32]. Measured air velocities on the breathing plane in the occupied zone reached maximum values 0.40 m/s for grille, 0.31 m/s for circular diffuser, and 0.21 m/s for duct diffuser. Average v_a values were measured 0.09 m/s, 0.10 m/s, and 0.11 m/s respectively. According to Figure 6, the grille and circular diffuser colour-plots indicate the

highest draught risk in the occupied zone border and room perimeter area. In the occupied zone, there is one area where duct diffuser reaches 0.21 m/s and drops to Category III. The rest of occupied zone well fulfils second Category.

Considering all the variation provided in Figure 1, the layout of internal heat gain sources or air terminals did not have a substantial impact on the results generally. We measured only three air distribution

solution in this study indicating the need to measure other possible solution. Measurements are highly needed because the result of ventilation effectiveness >1 for circular diffusers was impossible to predict. Similarly, increasing the number of extraction points from 1 to 6 in some cases decreased the performance (grille and circular diffuser) but in the case of duct diffusers enhanced the performance. Results are

promising, showing that ventilation effectiveness values equal or higher than 1 are possible. This allows not to increase the ventilation rate that may result in elevated draught risk and not to mention higher space demand or cost- and energy efficiency parameters. To sum up, the need for further research regarding ventilation effectiveness values is crucial, essentially in case of infection risk-based ventilation design.

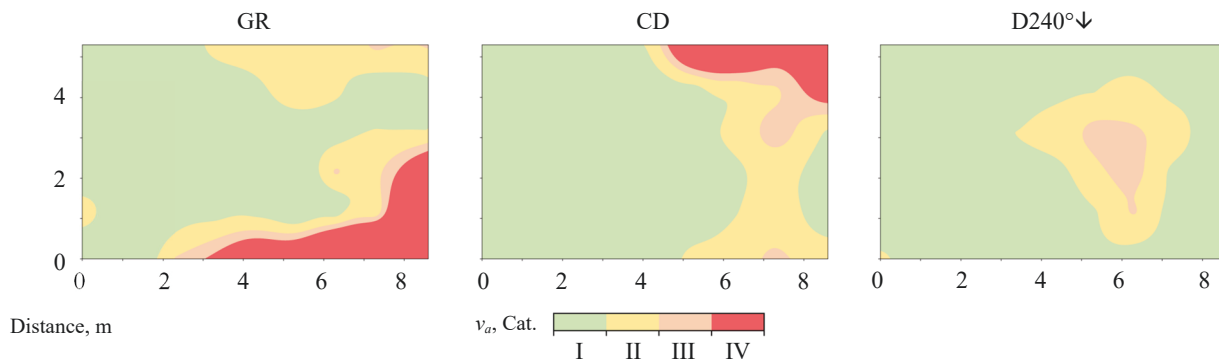


Figure 6. Results of measured air velocity (v_a) representing a mock-up classroom breathing plane colour-maps. Green stands for I Category (<0.10 m/s), yellow for II Category ($0.10\text{--}0.16$ m/s), light red for III Category ($0.16\text{--}0.21$ m/s), and dark red for IV Category (>0.21 m/s) during summer [32]. Grille (GR), circular diffuser (CD), and duct diffuser ($D240^\circ\downarrow$) are compared (for measurement grid and equipment, see Figure 2).

3 Conclusions

In this paper, ventilation effectiveness indices including air change efficiency (ε^a) and contaminant removal effectiveness (ε^c) simultaneously with air velocity were studied in a mock-up classroom. Supply grille, circular diffuser, and duct diffuser with single and six extract air terminal layouts were compared. We propose point source ventilation effectiveness (ε_b) approach to be calculated as an average of the two or more measurements with different contaminant source locations as a conservative efficiency value allowing to recalculate the fully mixing airflow rate to the actual ventilation air distribution solution. Further research regarding ventilation effectiveness values measured with point source would be crucial. Therefore, more combinations for air terminals, temperature amplitudes, room layouts etc must be investigated. In conclusion, we found that:

- There was no good correlation between ε^a and ε^c . Local ventilation effectiveness of contaminant removal showed that fully mixing is not a case with a point source, although air change efficiency determined with equally distributed source showed fully mixing conditions.
- Circular diffuser showed surprisingly ventilation effectiveness values >1 whereas six extraction points did not always perform better than single extract.
- In the infection risk-based ventilation design with contaminant point source (Covid-19), point source ventilation effectiveness ε_b values can be used as a correction factor for mixing ventilation airflow rate.

Author Contributions: J.K., T.T. and A.M. conceived and designed the experiments. A.M., I.V. and M.K. prepared and conducted the measurements and analysed the data. K.-V.V. helped to visualise the results. J.K., A.M., R.S., I.V. and M.K. wrote this paper.

Funding: This research was supported by the Estonian Centre of Excellence in Zero Energy and Resource Efficient Smart Buildings and Districts, ZEBE (grant 2014-2020.4.01.15-0016) funded by the Euro-pean Regional Development Fund, by the Estonian Ministry of Education and Research and European Regional Fund (grant 2014-2020.4.01.20-0289), by the European Commission through the H2020 project Finest Twins (grant No. 856602), and by the Estonian Research Council grant (PSG409).

References

1. Duffield, T.J. School ventilation. Its effect on the health of the pupil. *Am. J. Public Health* **1927**, *17*, 1226–1229.
2. Toyinbo, O.; Shaughnessy, R.; Turunen, M.; Putus, T.; Metsämuuronen, J.; Kurnitski, J.; Haverinen-Shaughnessy, U. Building characteristics, indoor environmental quality, and mathematics achievement in Finnish elementary schools. *Build. Environ.* **2016**, *104*, 114–121.
3. d'Ambrosio Alfano, F.R.; Bellia, L.; Boestra, A.; van Dijken, F.; Ianniello, E.; Lopardo, G.; Minichiello, F.; Romagnoni, P.; da Silva, M.C.G. *Indoor Environment and Energy Efficiency in Schools*; Rehva, Federation of European Heating and Air-conditioning Associations, 2010;
4. Johnson, D.L.; Lynch, R.A.; Floyd, E.L.;

- Wang, J.; Bartels, J.N. Indoor air quality in classrooms: Environmental measures and effective ventilation rate modeling in urban elementary schools. *Build. Environ.* **2018**, *136*, 185–197.
5. Stafford, T.M. Indoor air quality and academic performance. *J. Environ. Econ. Manage.* **2015**, *70*, 34–50.
6. Simons, E.; Hwang, S.-A.; Fitzgerald, E.F.; Kielb, C.; Lin, S. The impact of school building conditions on student absenteeism in upstate New York. *Am. J. Public Health* **2010**, *100*, 1679–1686.
7. Wargocki, P.; Wyon, D.P. The effects of moderately raised classroom temperatures and classroom ventilation rate on the performance of schoolwork by children (RP-1257). *Hvac&R Res.* **2007**, *13*, 193–220.
8. Salthammer, T.; Uhde, E.; Schripp, T.; Schieweck, A.; Morawska, L.; Mazaheri, M.; Clifford, S.; He, C.; Buonanno, G.; Querol, X. Children's well-being at schools: Impact of climatic conditions and air pollution. *Environ. Int.* **2016**, *94*, 196–210.
9. Bakó-Biró, Z.; Clements-Croome, D.J.; Kochhar, N.; Awbi, H.B.; Williams, M.J. Ventilation rates in schools and pupils' performance. *Build. Environ.* **2012**, *48*, 215–223.
10. Wargocki, P.; Wyon, D.P. Providing better thermal and air quality conditions in school classrooms would be cost-effective. *Build. Environ.* **2013**, *59*, 581–589.
11. Mundt, M.; Mathisen, H.M.; Moser, M.; Nielsen, P. V Ventilation effectiveness: Rehva guidebooks. **2004**.
12. Batterman, S. Review and extension of CO₂-based methods to determine ventilation rates with application to school classrooms. *Int. J. Environ. Res. Public Health* **2017**, *14*, 145.
13. Chung, K.-C.; Hsu, S.-P. Effect of ventilation pattern on room air and contaminant distribution. *Build. Environ.* **2001**, *36*, 989–998.
14. ISO/TC 163; CEN/TC 89 EVS-EN ISO 12569:2017 Thermal performance of buildings and materials. *Determ. Specif. airflow rate Build. - Tracer gas dilution method* **2017**.
15. ISO/TC 146 ISO 16000-8:2007 Indoor air - Part 8: *Determ. local mean ages air Build. Charact. Vent. Cond.* **2007**.
16. Novoselac, A.; Srebric, J. Comparison of air exchange efficiency and contaminant removal effectiveness as IAQ indices. *Trans. Soc. Heat. Refrig. Air Cond. Eng.* **2003**, *109*, 339–349.
17. Mustakallio, P.; Kosonen, R. Indoor air quality in classroom with different air distribution systems. *Indoor Air* **2011**, 5–10.
18. Kosonen, R.; Mustakallio, P. Ventilation in classroom: a Case-study of the performance of different air distribution methods. In *Proceedings of the Proceedings of 10th REHVA World Congress-Clima*; 2010.
19. Lichtner, E.; Kriegel, M. Pathogen spread and air quality indoors-ventilation effectiveness in a classroom. **2021**.
20. Li, Y.; Leung, G.M.; Tang, J.W.; Yang, X.; Chao, C.Y.; Lin, J.Z.; Lu, J.W.; Nielsen, P.V.; Niu, J.; Qian, H. Role of ventilation in airborne transmission of infectious agents in the built environment-a multidisciplinary systematic review. *Indoor Air* **2007**, *17*, 2–18.
21. Zhang, J. Integrating IAQ control strategies to reduce the risk of asymptomatic SARS CoV-2 infections in classrooms and open plan offices. *Sci. Technol. Built Environ.* **2020**, *26*, 1013–1018.
22. Cao, G.; Awbi, H.; Yao, R.; Fan, Y.; Sirén, K.; Kosonen, R.; Zhang, J.J. A review of the performance of different ventilation and airflow distribution systems in buildings. *Build. Environ.* **2014**, *73*, 171–186.
23. Müller, D.; Kandzia, C.; Kosonen, R.; Melikov, A.K.; Nielsen, P.V. *Mixing Ventilation Guide on mixing air distribution design*; Rehva, Federation of European Heating and Air-conditioning Associations, 2013;
24. Kurnitski, J.; Kiil, M.; Wargocki, P.; Boerstra, A.; Seppänen, O.; Olesen, B.; Morawska, L. Respiratory infection risk-based ventilation design method. *Build. Environ.* **2021**, *206*, 108387.
25. Nordic Ventilation Group; Rehva Technology and Research Committee COVID-19 Task Force Health-based target ventilation rates and design method for reducing exposure to airborne respiratory infectious diseases. *Rehva* **2022**, 6.
26. EVS/TC 27 EVS 906:2018 Ventilation for non-residential buildings. *Perform. Requir. Vent. room-conditioning Syst. Est. Natl. Annex EVS-EN 16798-3:2017* **2017**.
27. Onset Computer Corporation HOB0 MX1102A data logger Available online: <https://www.onsetcomp.com/products/data-loggers/mx1102a/>.
28. Testo SE & Co. KGaA Testo 440 dP datasheet Available online: <https://www.testo.com/en-US/testo-440-dp/p/0560-4402>.
29. KERN & SOHN GmbH Kern FKB datasheet Available online: <https://www.kern-sohn.com/en/FKB>.
30. Dantec Dynamics A/S ComfortSense Probes Available online: <https://www.dantecdynamics.com/product-category/thermal-comfort/comfortsense-probes/>.
31. CEN/TC 156 EVS-EN 16798-3:2017 Energy performance of buildings. *Vent. Build. - Part 3 Non-resid. Build. - Perform. Requir. Vent. room-conditioning Syst. (Modules M5-1, M5-4)* **2017**.
32. 156, C. 16798-1. Energy performance of buildings—Ventilation for buildings—Part 1. *Therm. Environ. Light. Acoust. M1-6.(16798-1)* **2019**.